

M.TREPCZYŃSKA-LENT\*

## POSSIBILITIES OF THE MATERIALS PROPERTIES IMPROVEMENT FOR THE CEMENTITE EUTECTIC BY MEANS OF UNIDIRECTIONAL SOLIDIFICATION

### MOŻLIWOŚCI POPRAWY WŁASNOŚCI UŻYTKOWYCH EUTEKTYKI CEMENTYTOWEJ METODĄ KRYSZALIZACJI ZORIENTOWANEJ

The paper brings the results of directional solidification of Fe-Fe<sub>3</sub>C eutectic alloy. The Bridgman method with vertical thermal gradient in conducted research was applied. Two values of rate was used for sample movement testing. One sample after solidification, was

immediately taken of the cooler. The distribution of thermal gradient in the alloy was determined. The value of thermal gradient in liquid at the solidification front was determined. On the samples, where cementite eutectic was oriented, interphase spacing  $\bar{\lambda}$  was measured. The results of the dependence between parameters  $v$  and  $\bar{\lambda}$  were presented. The research with application of optical microscope and computer programme to image analysis NIS-Elements was used.

*Keywords:* ledeburite, directional solidification, eutectic, structure, interphase spacing

W pracy przedstawiono rezultaty kierunkowej krystalizacji stopu eutektycznego Fe-Fe<sub>3</sub>C. Wykorzystano metodę Bridgmana z pionowym gradientem temperatury. Zastosowano dwie prędkości przemieszczania próbki. Jedną z próbek, po zrealizowaniu krystalizacji została zamrożona. Określono rozkład gradientu temperatury w stopie oraz wyznaczono wartość gradientu temperatury w cieczy na froncie krystalizacji. Na próbkach przeprowadzono pomiary odległości międzyfazowej  $\bar{\lambda}$ . Przedstawiono wyniki badań określających zależności pomiędzy parametrami  $v$  i  $\bar{\lambda}$ . W badaniach wykorzystano mikroskop optyczny oraz program do komputerowej analizy obrazu NIS-Elements.

#### 1. Introduction

Directional crystallization technology allows for alloys and improved properties. By controlling the crystallization front can get a crystalline structure with a preferred orientation of the external stress, and even strengthen the separation of phases. The main motivation in studying directional solidification of eutectic alloys is related to the possibility of obtaining composite material directly from the melt also known as in situ composites. Several studies have emphasized that this type of solidification process can produce materials with interesting mechanical properties. In situ eutectic alloys are interest for practical applications.

The solidification of regular eutectic alloys generally gives rise to lamellar, fibrous, broken lamellar or complex regular spacing's. The spacing of the lamellar or fibrous is typically very regular with a dispersion around an average value. The theoretical and experimental investigations are revealed for various eutectic alloys by many workers [1-4].

The eutectic directional solidification provides us microstructures with the simultaneous formation of two solid phases from one determined liquid, i.e. the phases of interest are obtained directly from the melt. The experimental studies

of alloys around the eutectic compositions of binary systems showed that in alloys frozen quickly, metastable phases are observed and formed with an eutectic morphology, being easily identified through metallographic analysis [5,6].

Most of the eutectic alloys of practical interest (Fe-C, Al-Si) are irregular. These and other irregular faceted-nonfaceted (f-nf) eutectics are widely employed in industry and are of greater practical importance than the regular eutectics [7-10].

Quasi-regular eutectic solidification near the highest value of  $g_{\alpha}$  which is over 0,4. They are characterized by lamellar-fibrous morphology. The typical feature of quasi-regular eutectics, is much about equal volumetric contribution of both eutectic phases and the growth of one of the phases in the shape of the wall crystal. Typical examples of this kind of eutectic can be seen in the Fe-Fe<sub>3</sub>C, Bi-Cd, Sb-Cu<sub>2</sub>Sb and Bi-Au<sub>2</sub>Bi alloys [11]. The characteristic of this group is that although they are in the anomalous (f-nf) class almost regular microstructures can be observed in these eutectics. In the quasi-regular eutectics the high degree of regularity may result from the fact that the faceted phase forms the matrix [12-14].

\* UNIVERSITY OF TECHNOLOGY AND LIFE SCIENCES, FACULTY OF MECHANICAL ENGINEERING, PROF. S. KALISKIEGO 7 AV, 85-796 BYDGOSZCZ, POLAND

## 2. Solidification of cementite eutectic

Cementite eutectic called ledeburite is generally defined as the eutectic structure formed between Fe/Fe<sub>3</sub>C. The term is used for both of the observed eutectic morphologies, *i.e.*, rod ledeburite and plate ledeburite. White iron structures generally form in a two stage process. First, plate-shaped dendrites of Fe<sub>3</sub>C nucleate at a few locations in the super cooled casting and spread throughout the liquid in a fanlike growth pattern. This plate dendrite formation of Fe<sub>3</sub>C occurred in both hypo- and hypereutectic alloys. In the hypoeutectic alloys, the first solid to form consisted of austenite dendrites, and the liquid between these dendrites was found to supercool significantly relative to the formation temperature of the white eutectic. Apparently, because of this super cooling, the first stage in the white iron formation was the growth of Fe<sub>3</sub>C plate dendrites, just as in hypereutectic alloys; only in the hypoeutectic alloys, the Fe<sub>3</sub>C dendrites grow around the pre-existing austenite dendrites. In the second stage for both hyper- and hypoeutectic alloys, a cooperative eutectic growth of austenite and Fe<sub>3</sub>C occurs on the sides of the primary Fe<sub>3</sub>C plates as the liquid between the plates solidifies, as Hillert and Subba Rao show schematically in Fig. 1. The cooperative eutectic growth occurs at right angles to the primary Fe<sub>3</sub>C plates, with the morphology being the very well-defined rod eutectic microstructure which is a dominant characteristic of white cast iron structures. In their model of the growth process, the initial edgewise growth (not shown on Fig. 1a) is a noncooperative growth of primary Fe<sub>3</sub>C dendrites leading the growth front [15].

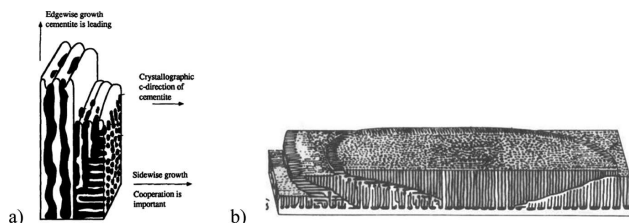


Fig. 1. Model of the structure of ledeburite growth by Hillert and Rao [15,16]

During the side eutectic growth ( $x$  direction) the area of undercooling concentration of the liquid solution comes into being that leads to the destabilization of the front, which changes from the planar into cellular one. The growth of the cells leads to carbon enrichment in the intercellular niches, in which cementite can crystallize. Adjacent lamellar cementite shallows join together, the austenite shallow becomes distributed, plate eutectic changes into fibrous eutectic. During the further side growth of eutectic grains only fibrous eutectic still crystallizes. According to the observations, cementite eutectic changes into either continuous carbides phase with austenite inclusions interpolation of various degree of dispersal, or plate structure that consists of the austenite and cementite plates (Fig. 1.) [16-19].

## 3. Interphase spacing in eutectic

Figure 2a is a schematic diagram of a regular lamellar eutectic structure which forms under steady-state directional solidification conditions for  $\alpha, \beta$  phase [20].

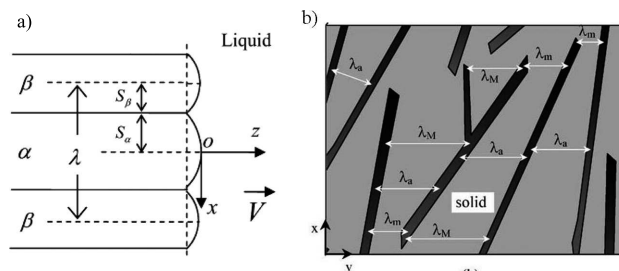


Fig. 2. a) A schematic diagram of a lamellar structure [20], b) The schematic illustration of the irregular growth, and interflake measurements on the longitudinal sections [8]

One of modelling of eutectic growth was given by Jackson and Hunt [21], why set up a mathematical model for stable growth of a regular eutectic with an isothermal growing interface, obtaining  $\lambda^2 v = \text{const}$ , where  $\lambda$  is the interphase spacing,  $v$  is the growth rate.

As can be seen in Fig.2b. the actual average spacing of irregular eutectic  $\lambda_a$ , is larger than extreme spacing  $\lambda_e$ .  $\lambda_a$  is close to the arithmetic average between minimum spacing,  $\lambda_m$  and maximum spacing  $\lambda_M$ .

## 4. Research material and experimental procedure

Pre-study research was conducted to obtain an alloy of Fe-C with 4,3% contents of carbon. The obtained samples were a starting material to lead the research on directional solidification of ledeburite. Armco iron and graphite electrodes with spectral purity were prepared as burden materials to the research. Initial melting was done in Balzers – type vacuum heater, in the conditions of backing vacuum. The smelt was subsequently degased under argon. The alloy was poured into four bar-shaped chills with a diameter  $\varnothing 12\text{mm}$ . From prepared bars the samples of  $\varnothing 5 \times 100\text{mm}$  were cut and then grinded. The directional solidification of the alloy can be realized by many sorts of equipment. In the conducted tests Bridgman's method with vertical temperature gradient was applied. It means that the whole metal is melted and then the form is continuously pulled out of the heater straight to the cooling centre. The machine consists of three main assemblies: a) resistor heating furnace, b) cooler, c) drive mechanism and additional supportive elements like power supply set, micro-processor supervising high temperature stabilization with an accuracy of  $\pm 2^\circ\text{C}$  and required scope of crucible movements rates.

## 5. Measurement of growth rates and thermal gradients

Kanthal Super resistance wire winding is a heating element which ensures high temperature inside the furnace. A cooler is built of two copper coats that takes care of continuous flow of water led to the thermostat. The space between internal coat and stall bar was fulfilled with low-melting alloy Ga-In-Sn with boiling high temperature. This alloy was used to eliminate gas gap between the crucible and a cooler and, as a result, to increase the temperature gradient in liquid metal at the front of solidification. In the upper part of alumina tube in upper head the double pipe of Al<sub>2</sub>O<sub>3</sub> with thermal element

Pt40Rh-Pt20Rh was installed. It allows to record the temperature of liquid metal alongside its moving route, namely  $T(x)$  where  $x$  is the distance from the cooler, as shown in Figure 3. On the basis of these data the curve of temperature uniformity was obtained and next, after numerical differentiation, the curve  $dT/dx$  (the uniformity of thermal gradient in the alloy) was determined. By using isotherm dividing liquid phase from solid one, the value of thermal gradient in the liquid at the front of solidification from the curve  $dT/dx$ , which is  $G = 33,5 \text{ K/mm}$  ( $G = 335 \text{ K/cm}$ ).

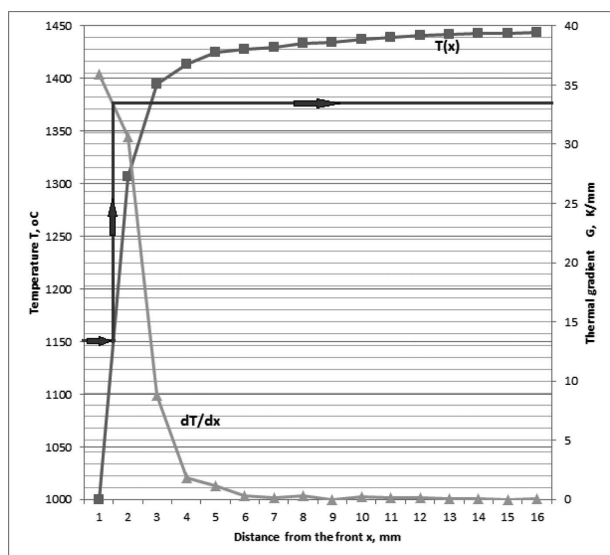


Fig. 3. Diagram of thermal gradient distribution in the examined alloy

Directional solidification was conducted in the following way. The samples of the initial alloy were placed inside alumina shields with a trade name Trialit-Degussit from Friatec Company with an internal diameter  $\phi_w = 6 \text{ mm}$  and external diameter  $\phi_z = 10 \text{ mm}$  and with a length 100 mm. These samples were stuck to the furnace drawbar by the high-temperature Morgan glue. The bottom end of the alumina shield and drawbar was submerged into liquid alloy fulfilling the cooler. After furnace sealing and delivering purified argon to the chamber the power was switched on. After the temperature stabilized to the level of  $1450^\circ\text{C}$ , the drive mechanism was launched. Drawbar with the samples on it was moving with a constant rate in regard to the cooler. On the determined thermal gradient at the front of solidification which is  $G = 33,5 \text{ K/mm}$  the sample movement rate of  $v = 83,3 \mu\text{m/s}$  ( $300 \text{ mm/h}$ ) and  $v = 166,7 \mu\text{m/s}$  ( $600 \text{ mm/h}$ ) was applied. One of the samples after solidifying was immediately taken off the cooler (frozen). Fe-Fe<sub>3</sub>C eutectic samples were unidirectional solidified with a constant thermal gradient but two different growth rates in order to study the dependence of average interphase spacing  $\bar{\lambda}$ .

## 6. Results and discussions

After the process of directional solidification of eutectic alloy Fe-Fe<sub>3</sub>C with sample movement rate of  $v = 83,3 \mu\text{m/s}$  and  $v = 166,7 \mu\text{m/s}$  the bars were obtained. On their longitudinal sections – in the different distance from the axis the metallographic specimens were made. The specimens were polished and etched with a reagent nital. The Fig. 4. show

the structure of ledeburite in the areas of obtained directional eutectic. The structure of the sample which was moved with a rate of  $v = 83,3 \mu\text{m/s}$  and frozen (immediately removed from the cooler) did not have the area of oriented ledeburite eutectic. Hypereutectic structure areas also appeared, namely ledeburite with numerous preliminary cementite separations, shown in Figure 5.

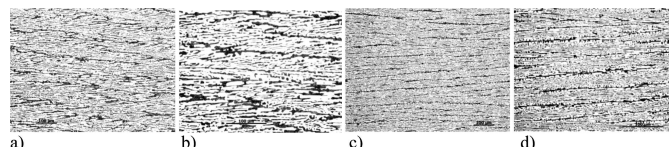


Fig. 4. Microstructure of directionally solidified Fe-Fe<sub>3</sub>C eutectic alloy on the longitudinal section of each samples,  $G = 33,5 \text{ K/mm}$ , a,b)  $v = 83,3 \mu\text{m/s}$ , c,d)  $v = 166,7 \mu\text{m/s}$

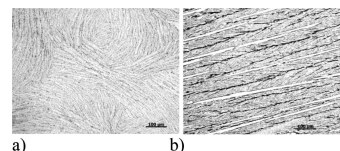


Fig. 5. Microstructure of a) eutectic, b) hypereutectic structure areas - samples after solidifying was frozen (immediately taken off the cooler),  $v = 83,3 \mu\text{m/s}$ ,  $G = 33,5 \text{ K/mm}$

### 6.1. The measurement of interphase spacing

On the samples, where the eutectic was versed, the measurements of geometrical parameter  $\bar{\lambda}$  were led. In the literature concerning volume metallography [22,23] various methods of interphase spacing measurement in eutectic are suggested. In this case, the average interphase spacing in oriented cementite eutectic was determined as a quotient of measure lines  $\sum L$  (perpendicular to the section) to the number of intersections  $f$  of these lines into cementite extraction  $\bar{\lambda} = \frac{\sum L}{f}$ . Geometric parameter was measured also by using computer application to picture analysis NIS-Elements. On the straight, which was draw perpendicularly to the axis and the straight section, the distances between cementite separations were measured, as shown in the Figure 6. Then, the calculations on the parameters were made with a use of Excel application. Approximately 240 lines, measured in at least 4 different distances from the face of the sample, in 5 successive longitudinal sections of each samples. The obtained values were verified statistically. The growth conditions and measurements for cementite eutectic are given in Tables 1. The dependence of average interphase spacing on distance from the face of the sample, growth rates, and as a function of the inverse square root of the growth rate are shown in Figs. 7,8, 9.

TABLE 1  
Growth conditions and measurements for cementite eutectic

Condition	$G$ K/mm	$v$ $\mu\text{m/s}$	$\bar{\lambda}$ $\mu\text{m}$	$\bar{\lambda} \cdot v^{1/2}$ $\mu\text{m}^{3/2} \text{ s}^{-1/2}$
1	33,5	83,3	$8,25 \pm 0,58$	75,3
2		166,7	$4,87 \pm 0,37$	62,9



Fig. 6. Measurement method of the number of intersections  $f$  of these lines into cementite extraction

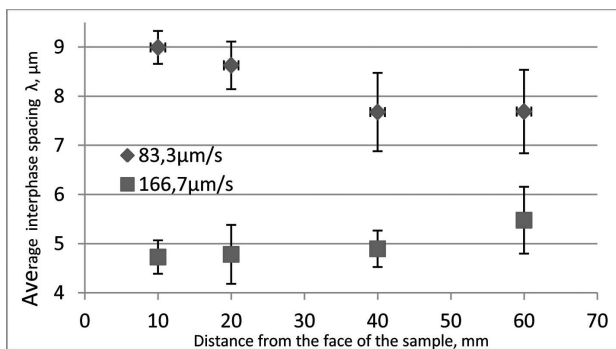


Fig. 7. The dependence of average interphase spacing  $\lambda$  on growth rates  $v$  at a constant  $G = 33,5$  K/mm

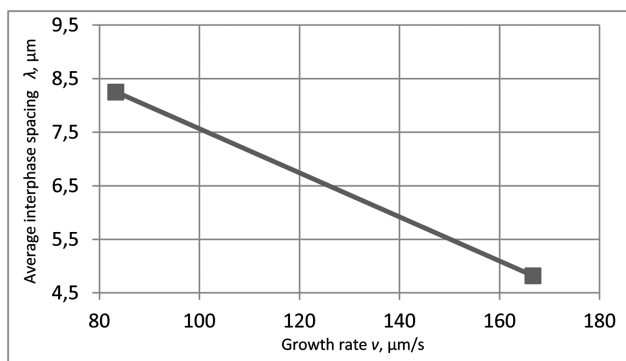


Fig. 8. The relationship between interphase spacing  $\lambda$  and eutectic growth rate  $v$  at a constant  $G = 33,5$  K/mm

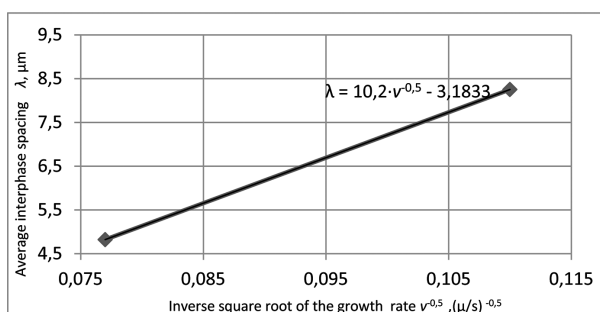


Fig. 9. Average interphase spacing as a function of the inverse square root of the growth rate,  $G = 33,5$  K/mm

## 7. Conclusion

The variation of interphase spacing  $\lambda$  according to the solidification parameters  $v$  and constant  $G$  for the Fe-Fe<sub>3</sub>C quasi-regular eutectic was investigated and relationships between them were obtained by statistical analysis.

These observation have led to the establishment of relationships of the right eutectic growth:  $\lambda = 10,2 \cdot v^{-0,5}$ ,  $\mu\text{m}$ . In the microstructure of the oriented cementite eutectic, a decrease in  $\lambda$  with increase of growth rate  $v$  was observed. The bulk growth rate  $\lambda \cdot v^{0,5}$  (Tab.1) was obtained by using experimental values and found be much higher than the Jones-Kurz value for lower  $G$  and smaller  $\lambda$  [6].

## Acknowledgements

The research were performed in the Department of Casting at the AGH University of Science and Technology in Cracow. The author wishes to express his gratitude to Prof. E. Guzik, Ph.D. E. Olejnik and M.Sc. A. Kolbus from Faculty of Alloy Engineering and Casting Composition.

## REFERENCES

- [1] P. Magnin, R. Trivedi, Eutectic growth: a modification of the Jackson and Hunt theory, *Acta Metall. Mater.* **39**, 453 (1991).
- [2] H. Kaya, M. Gündüz, E. Çadirli, O. Uzun, Effect of growth rate and lamellar spacing on microhardness in the directionally solidified Pb-Cd, Sn-Zn and Bi-Cd eutectic alloys, *Journal of Materials Science*, 1101, **39**, 21, 6571-6576 (2004).
- [3] E. Çadirli, M. Gündüz, The dependence of lamellar spacing on growth rate and temperature gradient in the lead-tin eutectic alloy, *Journal of Materials Processing Technology* **97**, 74-81 (2000).
- [4] W. Wołczyński, Concentration Micro-Field for Lamellar Eutectic Growth, *Defect and Diffusion Forum* **272**, 123-138 (2007).
- [5] I.A. Santos, A.A. Coelho, R.C. Araujo, C.A. Ribeiro, S. Gama, Directional solidification and characterization of binary Fe-Pr and Fe-Nd eutectic alloys, *Journal of Alloys and Compounds* **325**, 194-200 (2001).
- [6] H. Jones, W. Kurz, Relation of interphase spacing and growth velocity in Fe-C and Fe-Fe<sub>3</sub>C eutectic alloys, *Z. Metallkunde* **72**, 792 (1981).
- [7] W. Wołczyński, Lamella/Rod Transformation as described by the Criterion of Minimum Entropy Production, *International Journal of Thermodynamics* **13**, 35-42 (2010).
- [8] M. Gündüz, H. Kay, E. Çadirli, A. Özme, Interflake spacings and undercoolings in Al-Si irregular eutectic alloy, *Material Science and Engineering A* **3690**, 215-229 (2004).
- [9] E. Guzik, A model of irregular eutectic growth taking as an example the graphite eutectic in Fe-C alloys. *Dissertations Monographies 15*, Wyd. AGH, Kraków 1994.
- [10] E. Guzik, D. Kopyciński, Modelling structure parameters of irregular eutectic growth: Modification of Magnin-Kurz theory, *Metallurgical and Materials Transactions A* **37A**, 3057-3067, October 2006.
- [11] E. Fraś, *Krystalizacja metali WNT*, Warszawa 2003.
- [12] M.A. Savas, R.W. Smith, Quasi-regular growth: a study of the solidification of some high volume-fraction faceted phase anomalous eutectics, *Journal of Crystal Growth* **71**, 66-74 (1985).
- [13] M. Trepczyńska-Łent, Solidification of quasi-regular eutectic, *Archives of Foundry Engineering* **7**, 3, 171-178 (2007).
- [14] M. Trepczyńska-Łent, Solidification of ledeburite eutectic, *Archives of Foundry Engineering* **12**, SI 2, 71-74 (2012).

- [15] J.S. Park, J.D. Verhoeven, Directional solidification of white cast iron, *Metallurgical and Materials Transactions A* **27A**, 2328-2337 (1996).
- [16] Cz. Podrzucki, Cast iron. Structure, properties, application, ZG STOP, Cracow, 1991.
- [17] W. Wołczyński, E. Guzik, W. Wajda, D. Jędrzejczyk, B. Kania, M. Kostrzewa, CET in Solidifying Roll – Thermal Gradient Field Analysis, *Archives of Metallurgy and Materials* **57**, 105-117 (2012).
- [18] W. Wołczyński, W. Wajda, E. Guzik, Thermal Gradients Behaviour during the C-E Transition within Solidifying Massive Roll, *Solid State Phenomena* **197**, 174-179 (2013).
- [19] E. Fraś, M. Górny, An inoculation phenomenon in cast iron, *Archives of Metallurgy and Materials* **57**, 3, 767-777 (2012).
- [20] L. Liu, J.F. Li, Y.H. Zhou, Solidification of undercooled eutectic alloys containing a third element, *Acta Materiala* **57**, 1536-1545 (2009).
- [21] K.A. Jackson, J.D. Hunt, Lamellar and rod eutectic growth, *Trans. Metall. Soc. AIME* **236**, 1129 (1966).
- [22] J. Ryś, Metalografia ilościowa, Kraków, Wydawnictwo AGH, 1983.
- [23] E. Fraś, Krystalizacja żeliwa, Skrypt AGH nr 811, Kraków 1981.

This article was first presented at the VI International Conference "DEVELOPMENT TRENDS IN MECHANIZATION OF FOUNDRY PROCESSES", Inwałd, 5-7.09.2013

*Received: 20 January 2013.*